Electronic Supplementary Information

Second-shell modulation on porphyrin-like Pt single atom catalysts for boosting oxygen reduction reaction

Tayyaba Najam,[ab] Syed Shoaib Ahmad Shah,[c] Hanqing Yin,[d] Xin Xiao,[e] Shamraiz Talib,[f] Qianqian Ji,[a] Yonggui Deng,[g] Muhammad Sufyan Javed,[a] Jie Hu,[a] Ruo Zhao,[a] Aijun Du,[d] Xingke Cai, *[a] and Qiang Xu*[eh]

[a] Institute for Advanced Study, Shenzhen University, Shenzhen 518060, China. E-mail: cai.xingke@szu.edu.cn
[b] College of Physics and Optoelectronic Engineering, Shenzhen University, Shenzhen 518060, China.
[c] Department of Chemistry, School of Natural Sciences, National University of Sciences and Technology, Islamabad 44000, Pakistan.
[d] QUT Centre for Materials Science, Queensland University of Technology (QUT), 2 George Street, Brisbane, 4000, Australia.
[e] Shenzhen Key Laboratory of Micro/Nano-Porous Functional Materials (SKLPM), SUSTech-Kyoto University Advanced Energy Materials Joint Innovation Laboratory (SKAEM-JIL), Department of Chemistry and Department of Materials Science and Engineering, Southern University of Science and Technology (SUSTech), Shenzhen 518055, China. E-mail: xuq@sustech.edu.cn.
[f] Advanced Materials Chemistry Centre (AMCC), SAN Campus, Khalifa University, Abu Dhabi, P.O. Box 127788, United Arab Emirates
[g] College of Mechatronics and Control Engineering, Shenzhen University, Shenzhen 518060, PR China.
[h] Institute for Integrated Cell-Material Sciences (WPI-iCeMS), Kyoto University, Yoshida, Sakyo-ku, Kyoto 606-8501, Japan.

1. Experimental Section

1.1 XAFS Measurements

The X-ray absorption fine structure spectra (Pt L_3-edge) were collected at BL14W beamline in Shanghai Synchrotron Radiation Facility (SSRF). The storage rings of SSRF was operated at 3.5 GeV with a stable current of 200 mA. Using Si(111) double-crystal monochromator, the data collection were carried out in fluorescence mode using Lytle detector. All spectra were collected in ambient conditions. The data analysis was performed using the Athena/Artemis software packages.

1.2 Computational Method

All first-principle calculations were performed by the Vienna Ab-initio Simulation Package (VASP) considering of spin-polarization effect[1, 2]. The interaction between the ions and electrons were described by the projector-augmented wave (PAW)[3] method and the generalized gradient approximation in the Perdew−Burke−Ernzerhof (PBE)[4, 5] form was adopted. A DFT + D3 semiempirical correction was described via Grimme's scheme[6]. The cut-off energy was set to be 400 eV, and the force and energy convergence threshold was set to be 10^{-2} eV/Å and 10^{-5} eV, separately. The PtN4(P) active centers were constructed in a 6*6 graphene supercell by replacing certain carbon atoms with heterogeneous dopants. Vacuum layer of at least 20 Å was applied to avoid the interactions from adjacent periodical images in -z direction. The Gibbs free energy change (ΔG) of each elemental phase was calculated using the standard hydrogen electrode (SHE)[7].

The following are the four electron reaction steps for ORR processes[8]:

$$Pt^* + O_2\,(g) + H^+ + e^- \rightarrow PtOOH^* \quad (S1)$$

$$PtOOH^* + H^+ + e^- \rightarrow PtO^* + H_2O\,(l) \quad (S2)$$

$$PtO^* + H^+ + e^- \rightarrow PtOH^* \quad (S3)$$

$$PtOH^* + H^+ + e^- \rightarrow Pt^* + H_2O \quad (S4)$$

The Gibbs free energy difference for all of the above elementary steps (ΔG_{OOH*}, ΔG_{O*}, ΔG_{OH*}) that include an electron transfer is calculated by using the following equations:

$$\Delta G = \Delta E + \Delta ZPE - T\Delta S + \Delta G_U + \Delta Gp_H \quad (S5)$$

The energy difference between the free standing and adsorption states of reaction intermediates, changes in zero-point energies and entropy, are represented by ΔE, ΔZPE and ΔS. The adsorption energies of ΔE are derived directly from DFT calculations. The ΔZPE stands for change in zero-point energy, T stands for temperature (T = 298.15), and ΔS stands for entropy change, which are accomplished from the vibrational frequency. $\Delta G_U = -eU$, denotes the potential based on the SHE, where e and U are the number of electrons transferred. ΔG_{pH} stands for the Gibbs free energy correction of pH, which is determined using the formula: $\Delta G_{pH} = -k_B T In10^* pH$, where k_B represents the Boltzmann constant (1.380649×10^{-23} JK^{-1}) and T indicates a temperature of 298.15

k. The NIST database was used to obtain the vibrational frequencies and entropies of molecules in the gas phase.

The ΔG of four elementary steps for ORR processes can be defined as: $\Delta G_1 = \Delta G_{OOH*} - 4.92$, $\Delta G_2 = \Delta G_{O*} - \Delta G_{OOH*}$, $\Delta G_3 = \Delta G_{OH*} - \Delta G_{O*}$, $\Delta G_4 = \Delta G_{OH*}$.

The overpotential (η) used to further validate the catalytic activity of ORR would be derived using the following equations if the ΔG values of all four elementary steps are different:

$$\eta = \max \{\Delta G_1, \Delta G_2, \Delta G_3, \Delta G_4\} / e + 1.23 \qquad \text{(S6)}.$$

The exact adsorption energy of ClO_4^- was calculated as below:

$$\Delta E_{ads} = E(*ClO_4) - E(\text{surface}) - E(ClO_4^-) + E_{correction} \text{ (S7)},$$

where $E_{correction}$ contains the correction of the standard formation energy of $HClO_4$ and ClO_4^- of both gas and liquid phase and can be derived from experimental observation. Unfortunately, we didn't find their exact values yet it shouldn't affect the general trend of ClO_4^- adsorption on different SACs, because the correction represents only a constant shift when comparing the adsorption energies. Meanwhile, the energy of ClO_4^- ion was also inaccurate due to the limitation of our calculational methods, but it also has no influence on the trend because the error is constant as well.

2. Figures and Tables

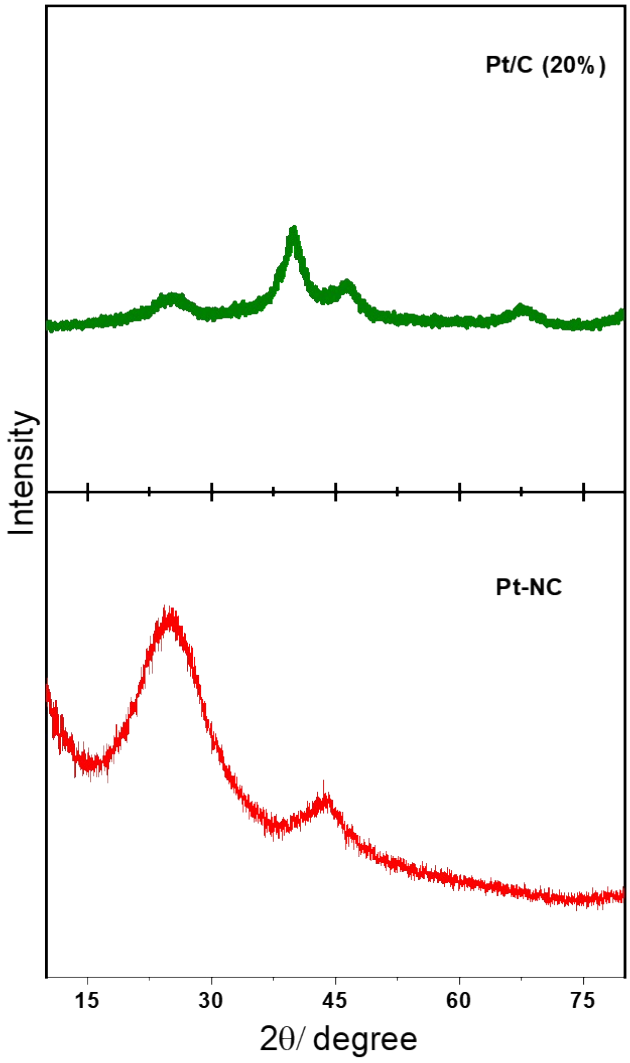

Fig. S1 XRD comparative analysis of commercial Pt/C (20%) and Pt-NC with a Pt content of 0.3wt%.

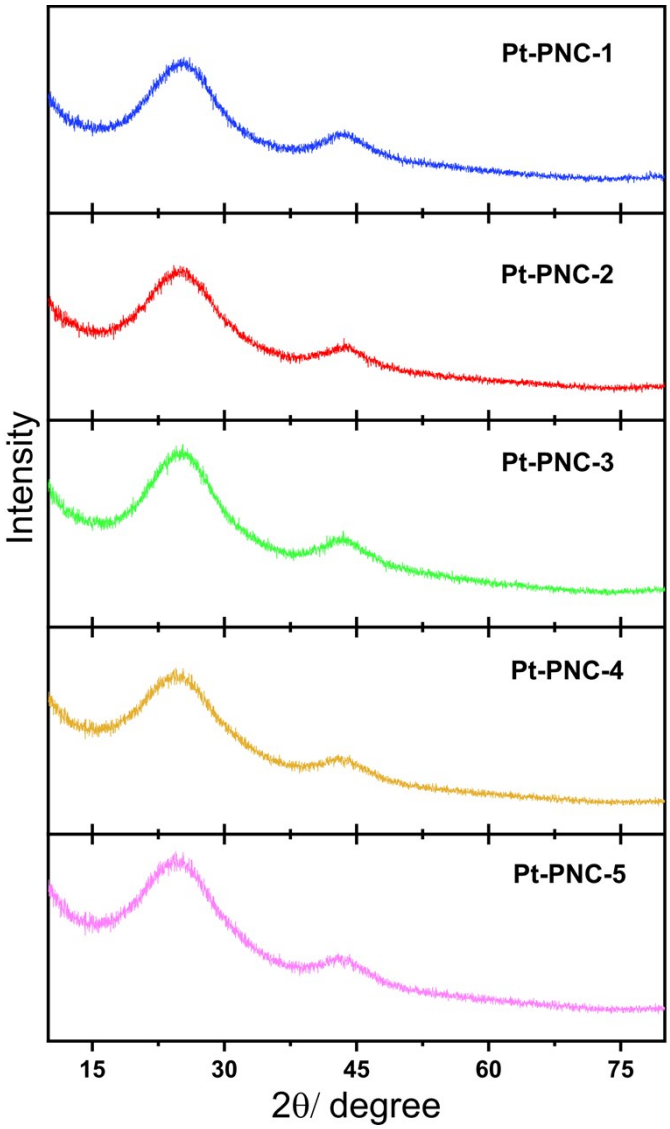

Fig. S2 XRD comparative analysis of Pt-PNC with varying Pt-loading.

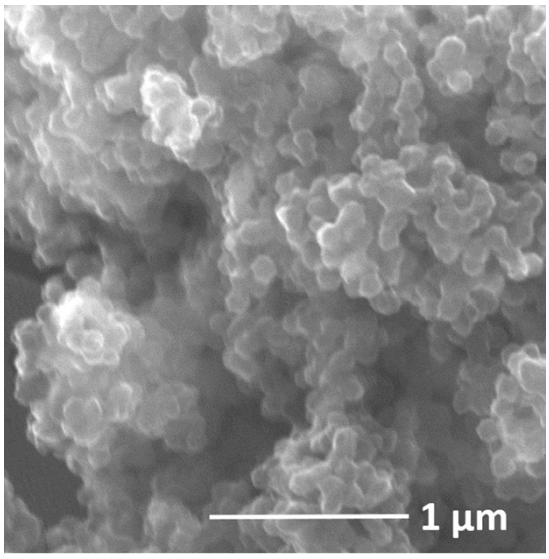

Fig. S3 Typical SEM image of Pt@ZIF-8.

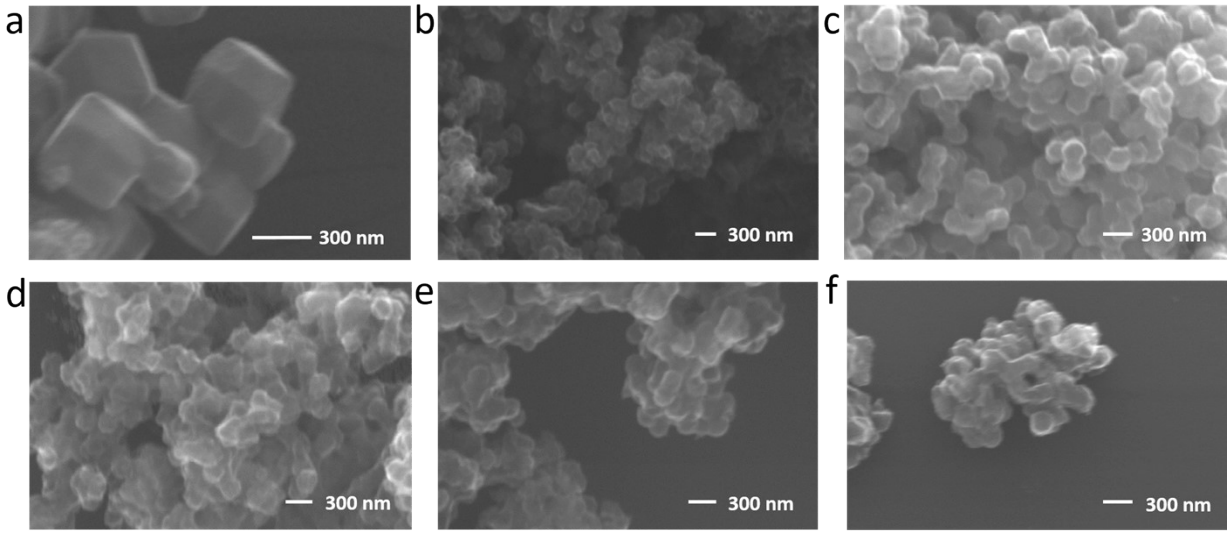

Fig. S4 SEM images of (a) PNC, (b) Pt-PNC-1, (c) Pt-PNC-2, (d) Pt-PNC-3, (e) Pt-PNC-4, (f) Pt-PNC-5.

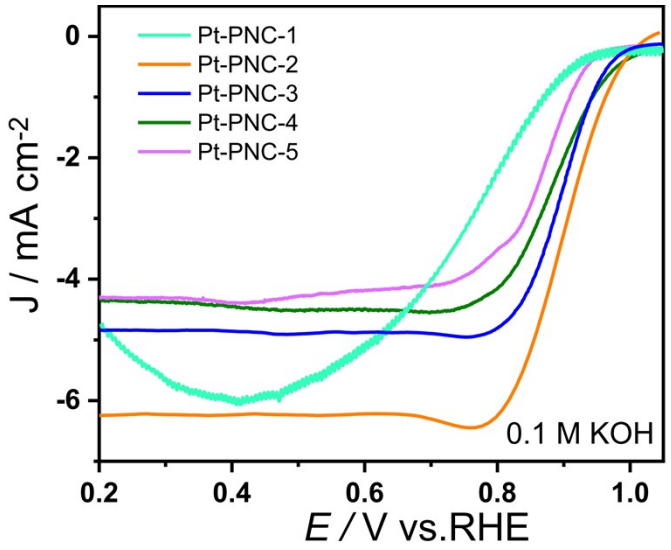

Fig. S5 ORR comparative study of Pt-PNC with varying Pt loading in 0.1 M KOH.

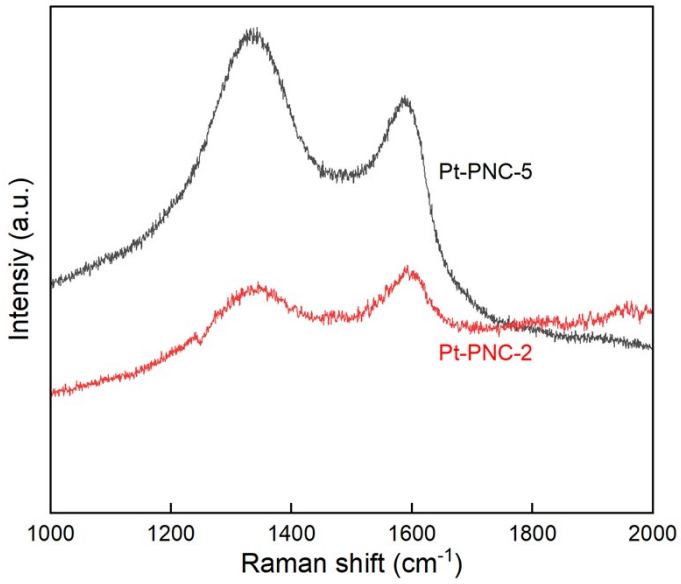

Fig. S6 Raman spectra of the catalysts determining the defects in the support. The I_D/I_G value has increased from 0.94 to 1.23 by increasing the Pt concentration doped inside from 0.22% to 0.33%.

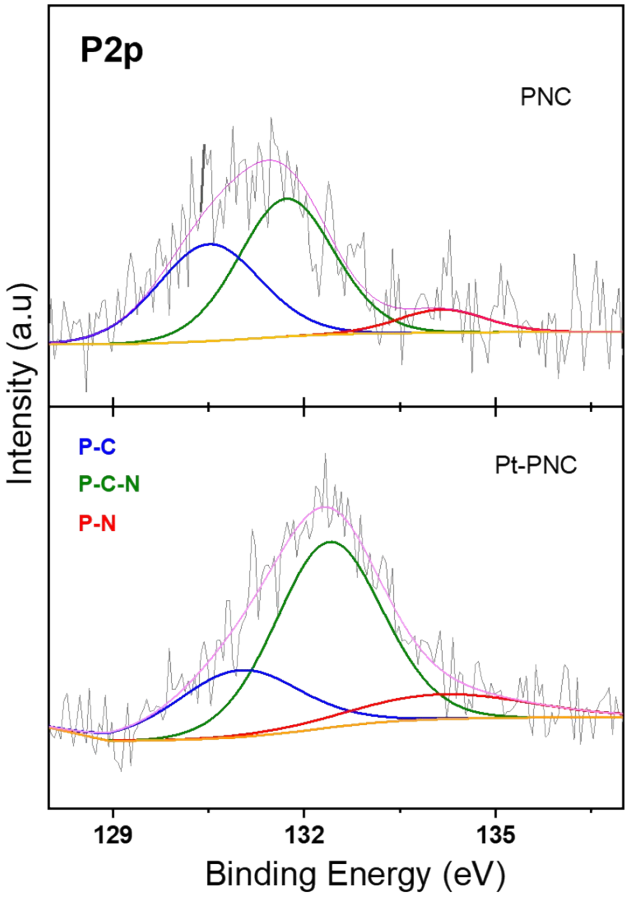

Fig. S7 XPS high resolution P2p spectrum.

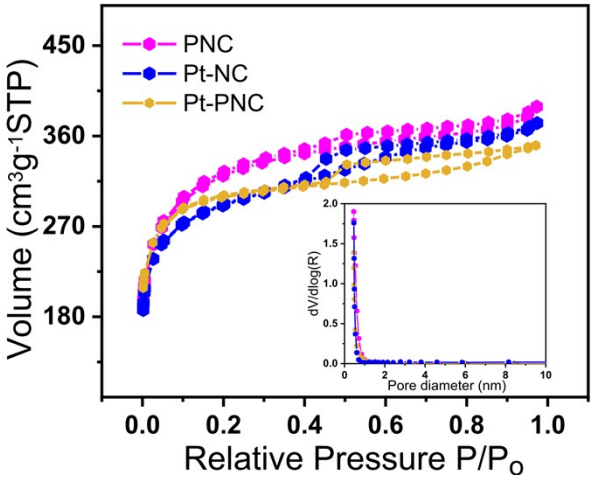

Fig. S8 N_2 adsorption-desorption isotherms (inset: pore size distribution).

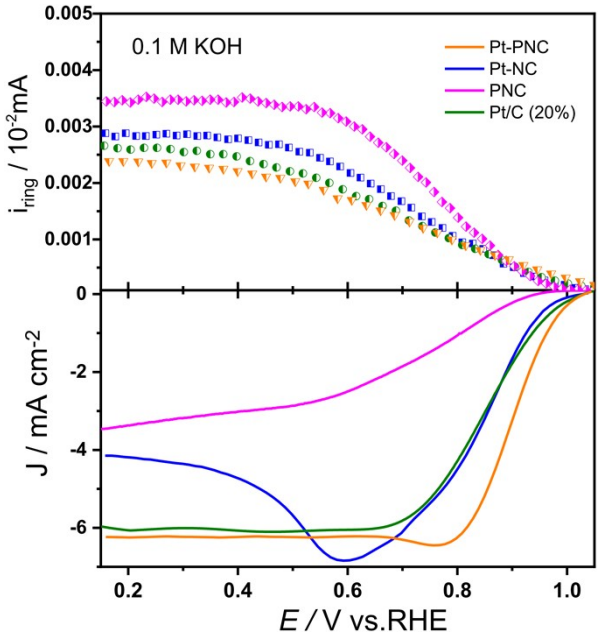

Fig. S9 RRDE performance of Pt-PNC, Pt-NC, PNC and Pt/C (20%) under 0.1 M KOH.

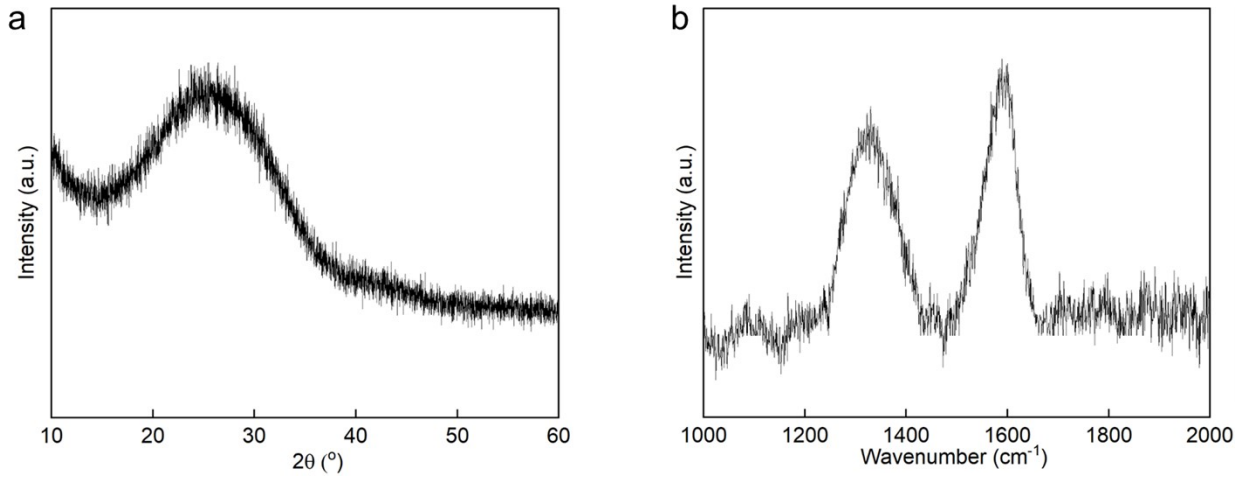

Fig. S10 Post-stability characterization of the Pt-PNC catalyst after 10000 cycles at the range of 0.6-1.2 V vs RHE in 0.1 M KOH solution. (a) XRD profile. (b) Raman spectrum.

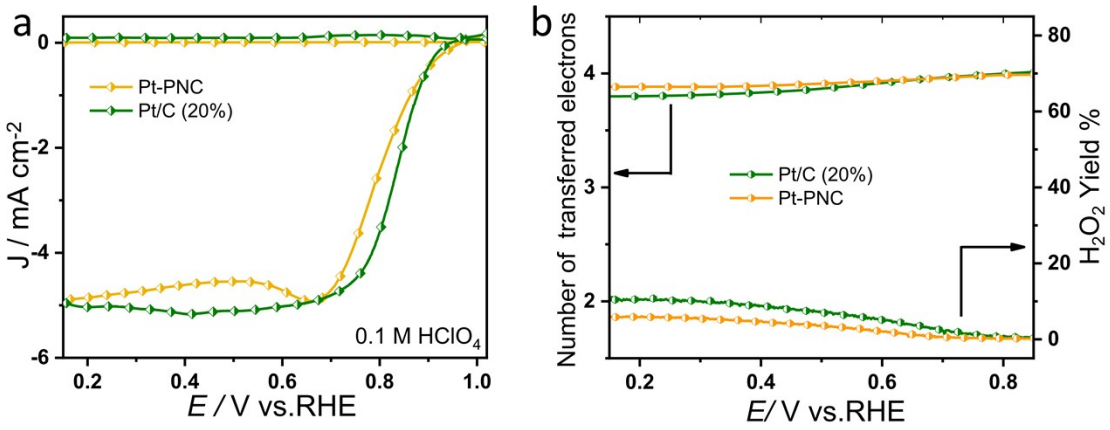

Fig. S11 (a) RRDE performance of Pt-PNC, and Pt/C (20%) under 0.1 M $HClO_4$. (b) Electron transferred number and peroxide% calculations.

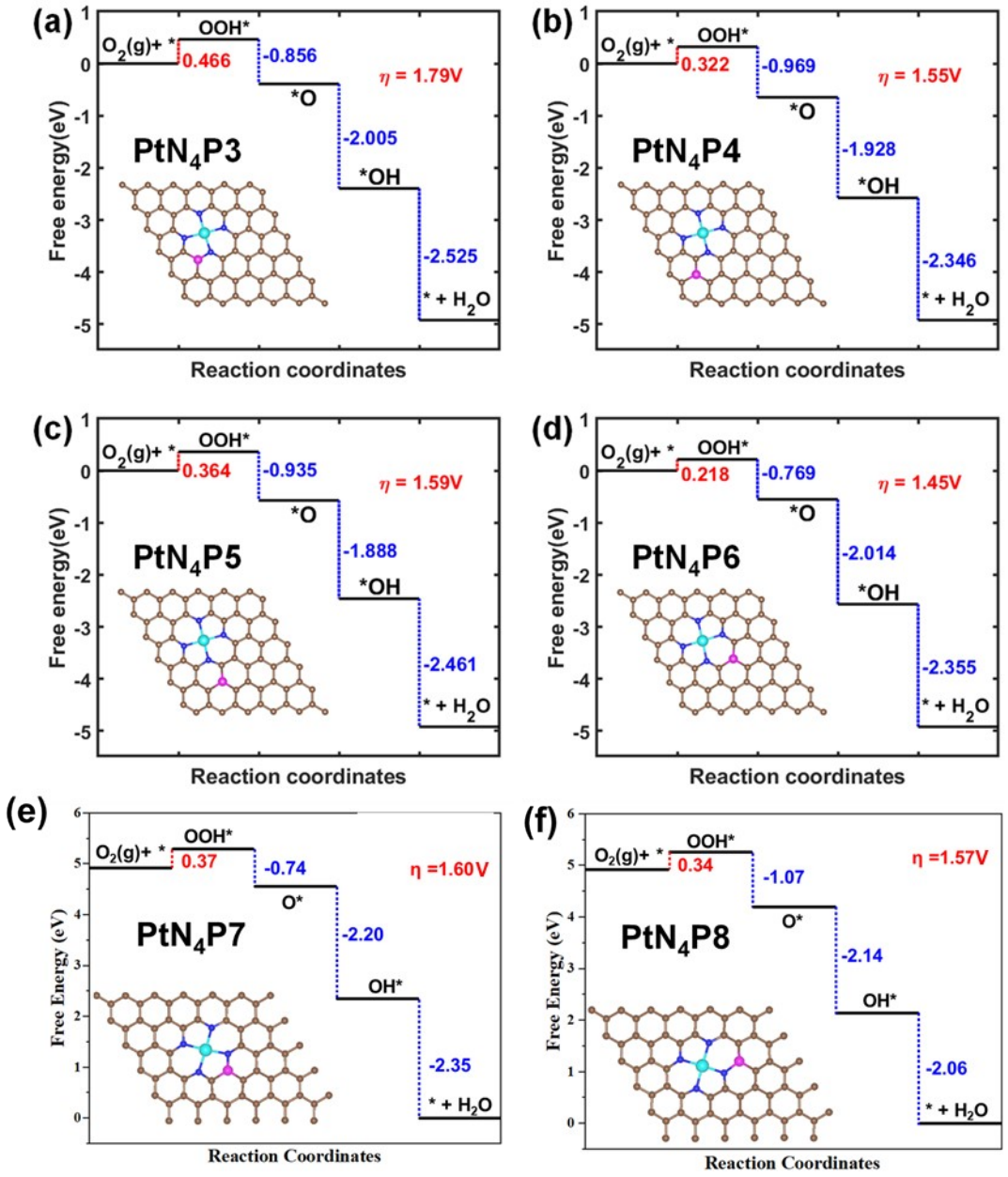

Fig. S12 Free energy diagrams and configurations of six structures studied in our theoretical calculations. Color map: brown-C; cyan-Pt; blue-N; purple-P.

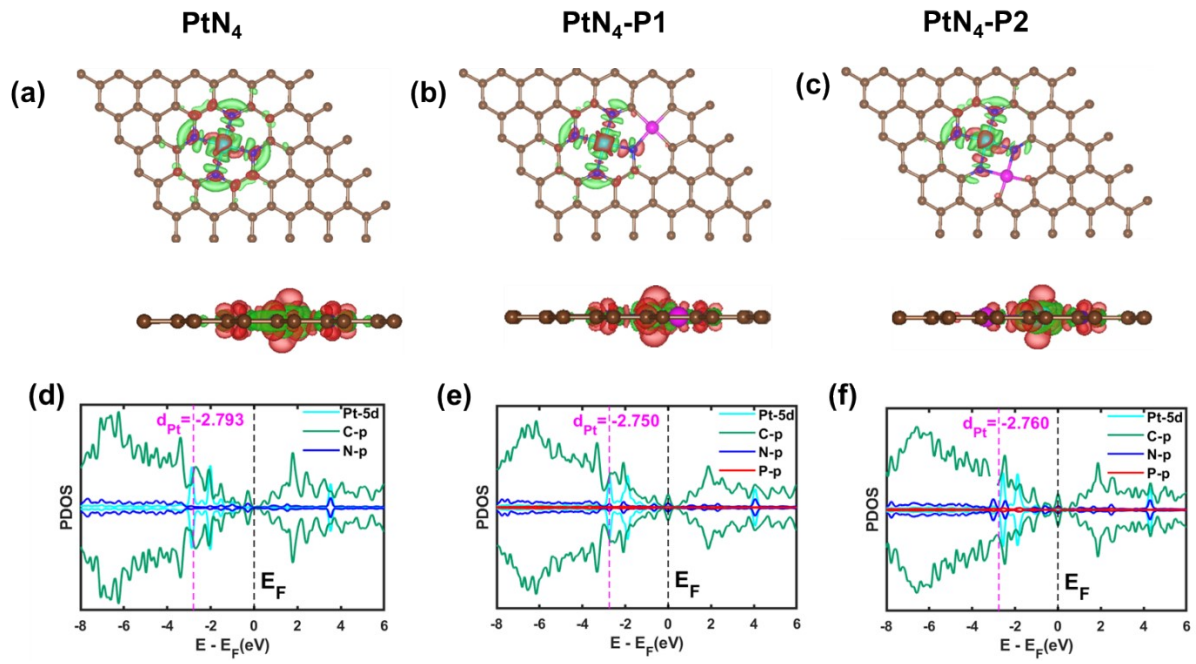

Fig. S13 (a-c) Top and side views of partial electron density differences (PEDD) of Pt atom anchored on the doped-graphene (PtN_4, PtN_4-P1, PtN_4-P2) monolayer. For the contour plots, the charge accumulation regions are rendered in blue while the charge depletion regions are shown in red. The contour value of the PEDD is ±0.005 a.u. (d-f) Calculated spin-polarized partial density of states (PDOS) of Pt atom anchored on the doped-graphene (PtN_4, PtN_4-P1, PtN_4-P2) monolayer. The Fermi level is fixed at the zero of energy and the d-band center (ε_d) is marked by the pink dashed line.

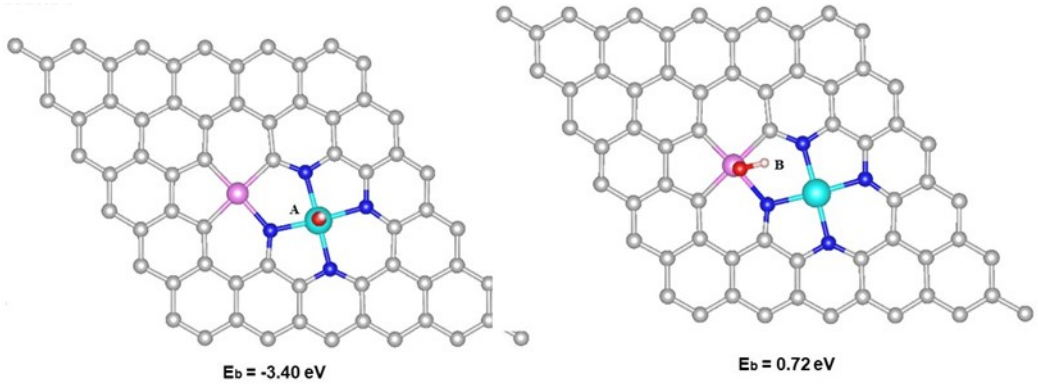

Fig. S14 Binding energies of OH-molecules on site-A (on the top of Pt-atom) and site-B (on the top of P-atoms).

The turn-over frequency (TOF) is estimated (Angew. Chem. Int. Ed. 2019, 58, 9640-9645) by the following question: $TOF=J_k \times N_e/(\omega_{Pt} \times C_{cat} \times N_A/M_{Pt})$, where J_k is the kinetic current density (A cm^{-2}), N_e is electron number per Coulomb 6.24 × 1018, ω_{pt} is the metal content in the catalyst, c_{cat} is the catalyst loading on the electrode, N_A is Avogadro constant 6.02 × 10^{23}, M_{Pt} is molar mass of Pt 195.1 g · mol^{-1}. As a result, we can get the relationship between the TOF and J_k to be TOF=4659.7 J_k in our Pt-PNC and Pt-NC catalysts.

Table S1. Pt wt% calculated from ICP analysis.

Catalyst	**wt%**
Pt-PNC-1	0.086
Pt-PNC -2	0.217
Pt-PNC -3	0.243
Pt-PNC -4	0.265
Pt-PNC -5	0.331

Table S2. Elemental composition as determined by XPS analysis.

Sample	**C** (atm%)	**N** (atm%)	**P** (atm%)	**Pt** (atm%)
PNC	91.79	7.66	0.55	-
Pt-PNC	95.13	4.11	0.45	0.31
Pt-NC	92.94	6.76	-	0.30

Table S3. EXAFS data fitting results of Pt-NC and Pt-PNC.

Sample	Path	CN	σ^2	Delta E_0	R(Å)	R-factor
Pt-NC	Pt-N/C	3.6(0.6)	0.0054(0.0011)	3.29(1.39)	1.99(0.02)	0.017
Pt-PNC	Pt-N/C	3.7(0.6)	0.0049(0.0012)	4.42(1.35)	2.01(0.02)	0.018

The following values were determined from fits of the standards and were then held constant for the fits shown above; "CN" is the coordination number; Three times the estimated standard deviation is shown in parentheses following each value. σ^2, Debye-Waller factor, 0.0029 Å^2; Interatomic distance = R (Å) (the bond length between central atoms and surrounding coordination atoms), R-factor (Goodness of fit) = $\Sigma k^6(\chi_o-\chi_c)^2/N_p$ where χ_o, χ_c are the observed and calculated EXAFS intensities, respectively and N_p is the number of points.

Table S4. Comparison of TOF in different catalysts for ORR

Catalysts	TOF (e^{-1} site^{-1} s^{-1})	Reference
Pt-PNC	15.0 (0.9 V)	This work
Pt-NC	8.1 (0.9 V)	This work
Pt/C	0.092 (0.9 V)	This work
Cu/CNT-8	0.72 (0.85 V)	46
Cu-N/C	~0.074 (0.85 V)	47
Co-N3 C1	0.46 (0.8 V)	48
Cu-N©C	~0.030 (0.85 V)	49
CPG-900	~0.052 (0.85 V)	50
Fe SAs-HP	5.99 (0.8 V)	51
Fe SACs	4.3 (0.8 V)	52
sur-FeN4-HPC	1.63 (0.8 V)	53

Table S5. Comparative study of Pt-PNC with reported SACs/DACs in acidic electrolytes based on precious and non-precious electrocatalysts.

Catalyst	Active Site	E_{onset} (V)	$E_{1/2}$ (V)	Electrolyte	Refs
Pt-PNC	Pt-N_4P	0.98	0.805	0.1 M $HClO_4$	This work
Pt_1-N/BP	Isolated Pt atoms anchored on N sites	-	0.76	0.1 M $HClO_4$	8
Pt_1@Fe-N-C	Pt_1-O_2-Fe_1-N_4	0.93	0.8	0.5 M H_2SO_4	9
Ru-N/G-750	Ru-oxo-N_4	0.89	0.75	0.1 M $HClO_4$	10

Ir SAC	IrN_4	0.97	0.864	0.1 M $HClO_4$	11
Fe ISAs/GHSs	Fe-N_x	1.05	0.87	0.1 M KOH	13
Fe SAs/N-C	Fe-N_4	-	0.798	0.1 M $HClO_4$	14
FeSA-G	Fe-N	0.95	0.804	0.1 M $HClO_4$	16
ZIF/MIL-10-900	Fe-N_4	-	0.78	0.1 M $HClO_4$	17
Fe_{SA}-N-C	Fe-N_4	0.93	0.776	0.1 M $HClO_4$	19
Fe-ZIF	Fe-N_4	-	0.85	0.5 M H_2SO_4	22
Co-N-C@F127	Co-N_4, Co-N_{2+2}	0.93	0.84	0.5 M H_2SO_4	28
Co-NC (1100)	Co-N_4		0.80	0.5 M H_2SO_4	31
Cu-SAs/N-C	Cu-N_4	0.83	-	0.1 M $HClO_4$	33
Zn-N-C-1	Zn-N_4	-	0.743	0.1 M $HClO_4$	36
Cr/N/C-950	Cr-N_4	-	0.773	0.1 M $HClO_4$	39
(FeCo)/N-C	(Fe-Co)N_6	1.06	0.863	0.1 M $HClO_4$	41
Co/Zn-NCNF	(Zn-Co)N_6	0.997	0.797	0.1 M $HClO_4$	43

Table S6. Comparative study of Pt-PNC with reported SACs/DACs in alkaline electrolytes based on precious and non-precious electrocatalysts.

Catalyst	**Active Site**	**E_{onset} (V)**	**$E_{1/2}$ (V)**	**Electrolyte**	**Zn-air battery (mW cm^{-2})**	**Refs**
Pt-PNC	Pt-N_4P	1.05	0.91	0.1 M KOH	247.8	This work
Ag-MnO_2	Isolated Ag atoms on MnO_2	0.95	-	1 M KOH	273.2	12
Fe ISAs/GHSs	Fe-N_x	1.05	0.87	0.1 M KOH	-	13

Fe SAs/N-C	$Fe-N_4$	-	0.91	0.1 M KOH	225	14
Fe-NC SAC	$Fe-N_x$	0.98	0.90	0.1 M KOH	-	15
Fe-NSDC	$Fe-N_x$	0.96	0.84	0.1 M KOH	225.1	18
Fe_{SA}-N-C	$Fe-N_4$	1.0	0.891	0.1 M KOH	-	19
S,N-Fe/N/C-CNT	$Fe-N_x$	-	0.85	0.1 M KOH	102.7	20
Fe-ISA/CN	$Fe-N_4$ with O_2 adsorbed on Fe-center	0.986	0.90	0.1 M KOH	-	21
CoN_4/NG	CoN_4	0.98	0.87	0.1 M KOH	115	23
EA-Co-900	Isolated Co-N Sites	-	0.84	0.1 M KOH	73	24
SCoNC	$Co-N_4$	-	0.91	0.1 M KOH	194	25
$Co-N_3C_1$@GC	$Co-N_3C_1$	0.913	0.854	0.1 M KOH	225	26
CoSAs/PTF-600	$Co-N_4$	-	0.808	0.1 M KOH	-	27
NC-Co-SA	$Co-N_x$	1.0	0.87	1 M KOH	20.9	29
CoSAs/N-C(900)	$Co-N_2$	0.982	0.881	0.1 M KOH		30
Cu ISAS/NC	CuN_3-defective	-	0.92	0.1 M KOH	280	32
Cu-SAs/N-C	$Cu-N_4$	0.99	0.895	0.1 M KOH	-	33
Cu-N-C	CuN_2, CuN_4	-	0.869	0.1 M KOH	-	34
Mn/C-NO	$Mn-N_3O_1$	-	0.86	0.1 M KOH	120	35
Zn-N-C-1	$Zn-N_4$	-	0.873	0.1 M KOH	-	36
SA-Zn-NHPC	$Zn-N_4$	1.00	0.87	0.1 M KOH	-	37
NiN_4-C	$Ni-N_4$	~0.97	~0.86	0.1 M KOH	-	38
Fe-NiNC-50	Fe-Ni	1.0	0.85	0.1 M KOH	220	40
Zn/CoN-C	$(Zn-Co)N_6$	1.004	0.861	0.1 M KOH	230	42
Zn, $Co-N_x$-C-Sy	Zn, $Co-N_6$-C-S	-	0.893	0.1 M KOH	150	44

CoNi-SAs/NC	$(Ni\text{-}Co)N_6$	0.88	0.76	0.1 M KOH	101.4	45

References

1 G. Kresse, J. Hafner, *Phys. Rev. B.*, 1993,**47**, 558.

2 G. Kresse, J. Furthmüller, *Phys. Rev. B*, *1996,* **54**, 11169.

3 P. E. Blöchl, *Phys. Rev. B*, *1994,* **50**, 17953.

4 J.Perdew, J. Chevary, S. Vosko, K. Jackson, M. Pederson, D. Singh, C. Fiolhais, *Phys. Rev. B*, *1992,* **46**, 6671.

5 J. P. Perdew, Y. Wang, *Phys. Rev. B*, *1992,* **45**, 13244.

6 S.Grimme, *J. Comput. Chem*, *2006,* **27**, 1787-1799.

7 J. Nørskov, J. Rossmeisl, A. Logadottir, L. Lindqvist, J. R. Kitchin, T. Bligaard, and H. Jónsson, *J. Phys. Chem. B*, *2004,* **108**, 17886-17892.

8 J. Liu, M. Jiao, L. Lu, H. M. Barkholtz, Y. Li, Y. Wang, L. Jiang, Z. Wu, D.-j. Liu, L. Zhuang, C. Ma, J. Zeng, B. Zhang, D. Su, P. Song, W. Xing, W. Xu, Y. Wang, Z. Jiang and G. Sun, *Nat. Commun.*, 2017, **8**, 15938.

9 X. Zeng, J. Shui, X. Liu, Q. Liu, Y. Li, J. Shang, L. Zheng and R. Yu, *Adv. Energy Mater.*, 2018, **8**, 1701345.

10 C. Zhang, J. Sha, H. Fei, M. Liu, S. Yazdi, J. Zhang, Q. Zhong, X. Zou, N. Zhao, H. Yu, Z. Jiang, E. Ringe, B. I. Yakobson, J. Dong, D. Chen and J. M. Tour, *ACS Nano*, 2017, **11**, 6930-6941.

11 M. Xiao, J. Zhu, G. Li, N. Li, S. Li, Z. P. Cano, L. Ma, P. Cui, P. Xu, G. Jiang, H. Jin, S. Wang, T. Wu, J. Lu, A. Yu, D. Su and Z. Chen, *Angew. Chem. Int. Ed.*, 2019, **58**, 9640-9645.

12 S. Ni, H. Zhang, Y. Zhao, X. Li, Y. Sun, J. Qian, Q. Xu, P. Gao, D. Wu, K. Kato, M. Yamauchi and Y. Sun, *Chem. Eng. J.*, 2019, **366**, 631-638.

13 X. Qiu, X. Yan, H. Pang, J. Wang, D. Sun, S. Wei, L. Xu and Y. Tang, Adv. Sci., 2019, 6, 1801103.

14 Z. Yang, Y. Wang, M. Zhu, Z. Li, W. Chen, W. Wei, T. Yuan, Y. Qu, Q. Xu, C. Zhao, X. Wang, P. Li, Y. Li, Y. Wu and Y. Li, *ACS Catal.*, 2019, **9**, 2158-2163.

15 L. Zhao, Y. Zhang, L.-B. Huang, X.-Z. Liu, Q.-H. Zhang, C. He, Z.-Y. Wu, L.-J. Zhang, J. Wu, W. Yang, L. Gu, J.-S. Hu and L.-J. Wan, *Nat. Commun.*, 2019, **10**, 1278.

16 Y. Cheng, S. He, S. Lu, J.-P. Veder, B. Johannessen, L. Thomsen, M. Saunders, T. Becker, R. De Marco, Q. Li, S.-z. Yang and S. P. Jiang, *Adv. Sci.*, 2019, **6**, 1802066.

17 X. Xu, Z. Xia, X. Zhang, R. Sun, X. Sun, H. Li, C. Wu, J. Wang, S. Wang and G. Sun, *Appl. Catal., B: Environ.*, 2019, **259**, 118042.

18 J. Zhang, M. Zhang, Y. Zeng, J. Chen, L. Qiu, H. Zhou, C. Sun, Y. Yu, C. Zhu and Z. Zhu, *Small*, 2019, **15**, 1900307.

19 L. Jiao, G. Wan, R. Zhang, H. Zhou, S.-H. Yu and H.-L. Jiang, *Angew. Chem. Int. Ed.*, 2018, **57**, 8525-8529.

20 P. Chen, T. Zhou, L. Xing, K. Xu, Y. Tong, H. Xie, L. Zhang, W. Yan, W. Chu, C. Wu and Y. Xie, *Angew. Chem. Int. Ed.*, 2017, **56**, 610-614.

21 Y. Chen, S. Ji, Y. Wang, J. Dong, W. Chen, Z. Li, R. Shen, L. Zheng, Z. Zhuang, D. Wang and Y. Li, *Angew. Chem. Int. Ed.*, 2017, **56**, 6937-6941.

22 H. Zhang, S. Hwang, M. Wang, Z. Feng, S. Karakalos, L. Luo, Z. Qiao, X. Xie, C. Wang, D. Su, Y. Shao and G. Wu, *J. Am. Chem. Soc.*, 2017, **139**, 14143-14149.

23 L. Yang, L. Shi, D. Wang, Y. Lv and D. Cao, *Nano Energy*, 2018, **50**, 691-698.

24 J. Zhao, R. Qin and R. Liu, *Appl. Catal., B: Environ.*, 2019, **256**, 117778.

25 J. Wu, H. Zhou, Q. Li, M. Chen, J. Wan, N. Zhang, L. Xiong, S. Li, B. Y. Xia, G. Feng, M. Liu and L. Huang, *Adv. Energy Mater.*, 2019, **9**, 1900149.

26 X. Hai, X. Zhao, N. Guo, C. Yao, C. Chen, W. Liu, Y. Du, H. Yan, J. Li, Z. Chen, X. Li, Z. Li, H. Xu, P. Lyu, J. Zhang, M. Lin, C. Su, S. J. Pennycook, C. Zhang, S. Xi and J. Lu, *ACS Catal.*, 2020, **10**, 5862-5870.

27 J.-D. Yi, R. Xu, G.-L. Chai, T. Zhang, K. Zang, B. Nan, H. Lin, Y.-L. Liang, J. Lv, J. Luo, R. Si, Y.-B. Huang and R. Cao, *J. Mater. Chem. A*, 2019, **7**, 1252-1259.

28 Y. He, S. Hwang, D. A. Cullen, M. A. Uddin, L. Langhorst, B. Li, S. Karakalos, A. J. Kropf, E. C. Wegener, J. Sokolowski, M. Chen, D. Myers, D. Su, K. L. More, G. Wang, S. Litster and G. Wu, *Energy Environ Sci.*, 2019, **12**, 250-260.

29 W. Zang, A. Sumboja, Y. Ma, H. Zhang, Y. Wu, S. Wu, H. Wu, Z. Liu, C. Guan, J. Wang and S. J. Pennycook, *ACS Catal.*, 2018, **8**, 8961-8969.

30 P. Yin, T. Yao, Y. Wu, L. Zheng, Y. Lin, W. Liu, H. Ju, J. Zhu, X. Hong, Z. Deng, G. Zhou, S. Wei and Y. Li, *Angew. Chem. Int. Ed.*, 2016, **55**, 10800-10805.

31 X. X. Wang, D. A. Cullen, Y.-T. Pan, S. Hwang, M. Wang, Z. Feng, J. Wang, M. H. Engelhard, H. Zhang, Y. He, Y. Shao, D. Su, K. L. More, J. S. Spendelow and G. Wu, *Adv. Mater.*, 2018, **30**, 1706758.

32 Z. Yang, B. Chen, W. Chen, Y. Qu, F. Zhou, C. Zhao, Q. Xu, Q. Zhang, X. Duan and Y. Wu, *Nat. Commun.*, 2019, **10**, 3734.

33 Y. Qu, Z. Li, W. Chen, Y. Lin, T. Yuan, Z. Yang, C. Zhao, J. Wang, C. Zhao, X. Wang, F. Zhou, Z. Zhuang, Y. Wu and Y. Li, *Nat. Catal.*, 2018, **1**, 781-786.

34 F. Li, G.-F. Han, H.-J. Noh, S.-J. Kim, Y. Lu, H. Y. Jeong, Z. Fu and J.-B. Baek, *Energy Environ. Sci.*, 2018, **11**, 2263-2269.

35 Y. Yang, K. Mao, S. Gao, H. Huang, G. Xia, Z. Lin, P. Jiang, C. Wang, H. Wang and Q. Chen, *Adv. Mater.*, 2018, **30**, 1801732.

36 J. Li, S. Chen, N. Yang, M. Deng, S. Ibraheem, J. Deng, J. Li, L. Li and Z. Wei, *Angew. Chem. Int. Ed.*, 2019, **58**, 7035-7039.

37 N. Wang, Z. Liu, J.-Y. Ma, J. Liu, P. Zhou, Y. Chao, C. Ma, X. Bo, J. Liu, Y. Hei, Y. Bi, M. Sun, M. Cao, H. Zhang, F. Chang, H.-L. Wang, P. Xu, Z. Hu, J. Bai, H. Sun, G. Hu and M. Zhou, *ACS Sustainable Chem. Eng.*, 2020, **8**, 13813–13822.

38 Z. Cai, P. Du, W. Liang, H. Zhang, P. Wu, C. Cai and Z. Yan, *J. Mater. Chem. A*, 2020, **8**, 15012-15022.

39 E. Luo, H. Zhang, X. Wang, L. Gao, L. Gong, T. Zhao, Z. Jin, J. Ge, Z. Jiang, C. Liu and W. Xing, *Angew. Chem. Int. Ed.*, 2019, **58**, 12469-12475.

40 X. Zhu, D. Zhang, C.-J. Chen, Q. Zhang, R.-S. Liu, Z. Xia, L. Dai, R. Amal and X. Lu, *Nano Energy*, 2020, **71**, 104597.

41 J. Wang, Z. Huang, W. Liu, C. Chang, H. Tang, Z. Li, W. Chen, C. Jia, T. Yao, S. Wei, Y. Wu and Y. Li, *J. Am. Chem. Soc.*, 2017, **139**, 17281-17284.

42 Z. Lu, B. Wang, Y. Hu, W. Liu, Y. Zhao, R. Yang, Z. Li, J. Luo, B. Chi, Z. Jiang, M. Li, S. Mu, S. Liao, J. Zhang and X. Sun, *Angew. Chem. Int. Ed.*, 2019, **58**, 2622-2626.

43 J. Zang, F. Wang, Q. Cheng, G. Wang, L. Ma, C. Chen, L. Yang, Z. Zou, D. Xie and H. Yang, *J. Mater. Chem. A*, 2020, **8**, 3686-3691.

44 D. Liu, B. Wang, H. Li, S. Huang, M. Liu, J. Wang, Q. Wang, J. Zhang and Y. Zhao, *Nano Energy*, 2019, **58**, 277-283.

45 X. Han, X. Ling, D. Yu, D. Xie, L. Li, S. Peng, C. Zhong, N. Zhao, Y. Deng and W. Hu, *Adv. Mater.*, 2019, **31**, 1905622.

46 G. Han, X. Zhang, W. Liu, Q. Zhang, Z. Wang, J. Cheng, T. Yao, L. Gu, C. Du, Y. Gao, G. Yin, *Nature communications* 2021, *12*, 6335.

47 Q. Lai, Y. Zhao, J. Zhu, Y. Liang, J. He, J. Chen, *ChemElectroChem* 2018, *5*, 1822-1826.

48 X. Hai, X. Zhao, N. Guo, C. Yao, C. Chen, W. Liu, Y. Du, H. Yan, J. Li, Z. Chen, X. Li, Z. Li, H. Xu, P. Lyu, J. Zhang, M. Lin, C. Su, S. J. Pennycook, C. Zhang, S. Xi, J. Lu, *ACS Catal.* 2020, *10*, 5862-5870.

49 H. Wu, H. Li, X. Zhao, Q. Liu, J. Wang, J. Xiao, S. Xie, R. Si, F. Yang, S. Miao, X. Guo, G. Wang, X. Bao, *Energy & Environmental Science* 2016, *9*, 3736-3745.

50 J. Wang, K. Wang, F.-B. Wang, X.-H. Xia, *Nature communications* 2014, *5*, 5285.

51 P. Zhang, H.-C. Chen, H. Zhu, K. Chen, T. Li, Y. Zhao, J. Li, R. Hu, S. Huang, W. Zhu, Y. Liu, Y. Pan, *Nature communications* 2024, *15*, 2062.

52 Z. Jin, P. Li, Y. Meng, Z. Fang, D. Xiao, G. Yu, *Nature Catalysis* 2021, *4*, 615-622.

53 G. Chen, Y. An, S. Liu, F. Sun, H. Qi, H. Wu, Y. He, P. Liu, R. Shi, J. Zhang, A. Kuc, U. Kaiser, T. Zhang, T. Heine, G. Wu, X. Feng, *Energy & Environmental Science* 2022, *15*, 2619-2628.